BIOSYSTEMS ENGINEERING 188 (2019) 229–242

Available online at www.sciencedirect.com

ScienceDirect

journal homepage: www.elsevier.com/locate/issn/15375110

Research Paper

A machine vision system for early detection and prediction of sick birds: A broiler chicken model

Cedric Okinda [a], Mingzhou Lu [a], Longshen Liu [a], Innocent Nyalala [a], Caroline Muneri [b,c], Jintao Wang [a], Hailin Zhang [a], Mingxia Shen [a,*]

[a] College of Engineering, Laboratory of Modern Facility Agriculture Technology and Equipment Engineering of Jiangsu Province, Nanjing Agricultural University, Jiangsu 210031, PR China
[b] College of Veterinary Medicine, Nanjing Agricultural University, Nanjing, Jiangsu 210095, PR China
[c] Faculty of Veterinary Medicine and Surgery, Department of Veterinary Surgery, Theriogenology and Medicine, Egerton University, Njoro, Kenya

ARTICLE INFO

Article history:
Received 4 February 2019
Received in revised form
31 August 2019
Accepted 29 September 2019
Published online 12 November 2019

Keywords:
Poultry welfare
Shape descriptors
Posture
Mobility
Support vector machine

The occurrence of poultry diseases not only affects farm production economics but also leads to poor poultry welfare, food safety concerns, and zoonotic infections. Therefore, timely detection of these diseases is of paramount importance in poultry production. This study proposes a machine vision-based monitoring system for broiler chicken as they walk through a test area. Data were collected from two groups of broilers; control group and treatment group (inoculated intramuscularly with virulent Newcastle disease virus) housed in fully isolated chambers for comparative monitoring. The broilers were monitored by video surveillance for data labelling and depth camera for the automated health status classifier development. Feature variables were extracted based on 2D posture shape descriptors (circle variance, elongation, convexity, complexity, and eccentricity) and mobility feature (walk speed). A statistical analysis of the feature variables established that all investigated features were statistically significant ($p < 0.05$) with time after challenge in the treatment group. The earliest possible infection detection time was on the 4th day based on circle variance and elongation, and the 6th day based on eccentricity and walk speed. However, convexity and complexity could not provide early detection. Two sets of classifiers were then developed based on only the posture shape descriptors, and on all the feature variables, The Support Vector Machine (RBF-SVM) outperformed all the other models with an accuracy of 0.975 and 0.978 respectively. The proposed system can serve as an automatic broiler monitoring system by providing an early warning and prediction of an occurrence of disease continuously and non-intrusively.

* Corresponding author.
E-mail address: mingxia@njau.edu.cn (M. Shen).
https://doi.org/10.1016/j.biosystemseng.2019.09.015

Nomenclature

2D	Two dimensional
3D	Three dimensional
ANN	Artificial Neural Network
°C	Degree Celsius
CPU	Central Processing Unit
fps	Frames per Second
GB	Gigabyte
G_C	Control group
G_T	Treatment group
GHz	Gigahertz
HD	High Definition
IQR	Interquartile Range
MAT	Medial Axis Transform
mdl_1	Model 1, based on only the shape descriptors
mdl_2	Model 2, based on both the shape descriptors and walk speed
MOV	Movie Digital Video
NDV	Newcastle Disease Virus
p	Probability value (p-value)
PC	Personal Computer
PLF	Precision Livestock Farming
P_t	Extracted feature variables
RBF	Radial basis function
ROI	Region of Interest
S_t	2D posture shape descriptors
SVM	Support Vector Machine
SDK	Software Development Kit
USB	Universal Serial Bus
V2	Version 2
γ_c	Circle Variance
γ_E	Shape Elongation
γ_{cv}	Shape Convexity
γ_{cx}	Shape Complexity
γ_e	Shape Eccentricity
γ_s	Chicken walk speed

1. Introduction

There has been a rise in the consumption of poultry meat and poultry meat products in the recent years, with a projected increase within the next decade (Henchion, McCarthy, Resconi, & Troy, 2014). Consequently, global poultry production has significantly increased, with a production of about 117 Mt in 2016 (OECD-FAO, 2017). With the large-scale production and breeding of livestock, the production risks involved have also increased (Manning, Chadd, & Baines, 2007; Sims, 2008). The main challenge affecting poultry production is the frequent occurrence of poultry diseases (Huang, Wang, & Zhang, 2019; Zhuang, Bi, Guo, Wu, & Zhang, 2018; Zhuang & Zhang, 2019), which has often led to significant losses in a flock or loss of entire flocks (Rushton, Viscarra, Bleich, & McLeod, 2005). Furthermore, poultry diseases pose a severe threat to food safety if infected meat and products are ingested (Friel & Ford, 2015). Poultry diseases like the avian influenza virus are zoonotic and have led to several global pandemics (Peiris et al., 2016; Rushton et al., 2005). Additionally, according to Welfare Quality® (2009), animal health condition is a key indicator of good welfare practice. This study focuses on broiler chicken, which is currently the main contributor to poultry meat production (OECD-FAO, 2017).

The conventional mode for chicken disease detection is by visual observations and sound distinction by farmers and veterinarians (Huang et al., 2019; Zhuang et al., 2018; Zhuang & Zhang, 2019). However, in large-scale production, these methods of detection are time-consuming, subjective, labour-intensive, and fail to provide an early detection (Zhuang et al., 2018). Tablante (2013) and Butcher, Jacob, and Mather (1999) reported on common poultry diseases, visible signs of each infection, and the modes of prevention and control. Additionally, the Chicken Health Handbook by Damerow (2016) described how to identify sick birds by several methodologies based on observations such as behavioural changes, depressed bird look (posture), variation in egg production, comb appearance, droppings examination, and post-mortem examination.

Our study presents a posture and mobility evaluation to provide a technique for distinguishing between healthy and sick birds. Generally, infected poultry always have a distinctly different body posture compared to healthy poultry (Butcher et al., 1999; Damerow, 2016; Manning et al., 2007; Zhuang et al., 2018). Similarly, mobility is another important factor that has been used to examine the health condition of birds. A sick bird is often reluctant to walk for very long and will isolate itself and displays a depressed bird look/posture (Damerow, 2016). Furthermore, Paul-Murphy and Hawkins (2014) reported that a bird in pain has a decreased social interaction and will always seclude itself and remain stationary at a distance from the rest of the flock.

Several studies have reported different techniques based on machine vision to monitor various bio-responses and bioprocesses that indicate health conditions in broilers such as weight-gain, behaviours, mobility, posture, and activities. Weight-gain is vital information in livestock production. It is an indicator of body growth, feed conversion ratio, and market readiness (Wongsriworaphon, Arnonkijpanich, & Pathumnakul, 2015). The first two are indicators of good health and good animal welfare, while the latter is applied in supply chain management. Additionally, good animal welfare is characterised by good health and productivity. Thus, monitoring animal weight gain can be used to detect disease occurrences and other vitality issues for necessary countermeasures to be undertaken (Menesatti et al., 2014; Mortensen, Lisouski, & Ahrendt, 2016). Generally, mobility is always associated with walking or locomotion as it describes the quality or state of being mobile or ability to move. In poultry, immobility is often a sign of birds experiencing some discomfort (Paul-Murphy & Hawkins, 2014). These discomforts may be as a result of skeleton (leg) disorders (Bradshaw, Kirkden, & Broom, 2002), nutrition deficiencies (Bradshaw et al., 2002), and health conditions such as leg health and diseases (Butcher et al., 1999; Tablante, 2013). Additionally, Aydin (2017a) reported that sound birds walk significantly faster than unsound birds. Thus, an infection greatly affects the mobility characteristics of a bird. Chicken mobility and activeness have been used to assess the degree of lameness in

several studies (Aydin, 2017a; 2017b). Furthermore, lameness in broilers describes a range of injuries resulting from an infection or non-infective origin (Thorp & Duff, 1988). Aydin (2017b) established that inactivity is highly correlated to lameness. Furthermore, Aydin (2017a) reported that broiler walk speed, step frequency, step length, and body oscillations are statistically correlated to the level of lameness. Kristensen and Cornou (2011) developed an automated system that could identify deviations in activity levels in a group of broiler chicken. The study characterised the undisturbed activity levels by age and could provide notification in any activity deviation to detect potential problems in the flock.

As mentioned earlier, depressed-bird-look/posture observation is a popular technique to identify sick birds. Zhuang et al. (2018) presented a system that could analyse broiler posture for early detection of sick broilers based on chicken image skeleton features for images taken from the side. Additionally, Zhuang and Zhang (2019) developed a sick broiler detection system based on deep learning technique using the B1 broiler and PASCAL VOC2012 databases. Both systems successfully classified sick and healthy broilers. Aerial posture analysis has also been presented by Pereira et al. (2013) to assess broiler welfare condition by use of an overhead video camera to develop a comprehensive assessment system for broiler behavioural expressions.

Moving on from earlier studies that have been performed in disease detection in broilers by image processing techniques, for real farm implementation, overhead images would be most preferred due to the ease of camera positioning in large-scale farms and the least disturbance to the animals (Van der Stuyft, Schofield, Randall, Wambacq, & Goedseels, 1991). Additionally, overhead images pose a less arduous task of background removal. Currently, there is no literature on the analysis of overhead posture shape to detect disease occurrence in broilers. Thus, this study proposes a methodology based on a non-intrusive depth camera sensor and machine vision for early detection and prediction of sick broilers.

The primary objective of this study was to develop an auto-classification system that could discriminate between healthy and sick broilers. The specific objectives included developing: an efficient depth image processing algorithm, an effective and robust posture analysis algorithm for 2D shape geometric features extraction, an algorithm to compute the broiler walk speed, a classifier to establish a correlation of broiler feature variables to the health status, and the statistical relationships between the extracted feature variables with an infection exposure period. This proposed system could serve as a Precision Livestock Farming (PLF) system if applied in a practical farm scenario by providing support to the stockmen in the detection of avian diseases in broiler production.

2. Materials and methods

2.1. Experiment design and monitoring system setup

Experiments were conducted between January 2018 and March 2019 at Ping Du Poultry Farm of New Hope Liu He Limited Company, Qingdao, Shandong Province, China. Day-old Arbor Acres broilers were obtained from the farm's hatchery and were reared in fully isolated controlled environment chambers. The temperature was set at 34 °C at the start of the experiment and gradually decreased until 26 °C on the last day of the experiment. The humidity was set at 50% at the beginning of the experiment and was gradually increased to 80% on the final day of the experiment. The chamber floor was litter (50% sphagnum and 50% wood-shavings). Feeding was performed according to the study by Aydin (2017b), and anti-stress vitamins were also given at strategic periods. Water was given *ad libitum* during the experimental period. The lighting regime consisted of two dark periods, following the study by Mortensen et al. (2016), with the light periods having an approximate light intensity of 30 lx for the duration of the experiment.

In each chamber, a wooden test corridor of dimensions 2.50 m (length) by 0.50 m (width) by 0.50 m (height), a 3D Kinect camera for Windows V2 (Microsoft Corp., Washington, USA) and a HD video surveillance camera DS-2CD3T35-13 (HIKVISION) were pre-installed before the chickens were brought into the chambers. The Kinect camera was positioned 2.50 m above the ground and precisely at the centre of the testing corridor, as shown in Fig. 1. The Kinect camera was connected to an Intel core i5-4500U CPU, 4 GHz, 16 GB physical memory (Intel, Santa Clara, CA, USA), Microsoft Windows 10 PC installed with the Kinect for Windows Software Development Kit (SDK) via a USB port. Depth images (512 × 424 pixels) were acquired from the Kinect camera at 1 fps using MATLAB R2018a (The MathWorks Inc., Natick, MA) image acquisition toolkit. An infrared (IR) depth sensor was applied due to its invariance to variations in ambient light conditions (Kongsro, 2014; Okinda, Lu, Nyalala, Li, & Shen, 2018). Additionally, the surveillance camera was used to acquire videos (for observation, labelling, and verification) at 22 fps MOV format. Figure 2 shows clear broiler colour images for the top view and side view during the experiment.

At 21 days old, the birds were tagged (poultry feet tags, Geshifeng Company) and randomly divided into two groups of 20 birds each; a total of 280 broilers were used in this study. The first group was a treatment group (G_T) and was inoculated intramuscularly with 200 μl virulent Newcastle Disease Virus

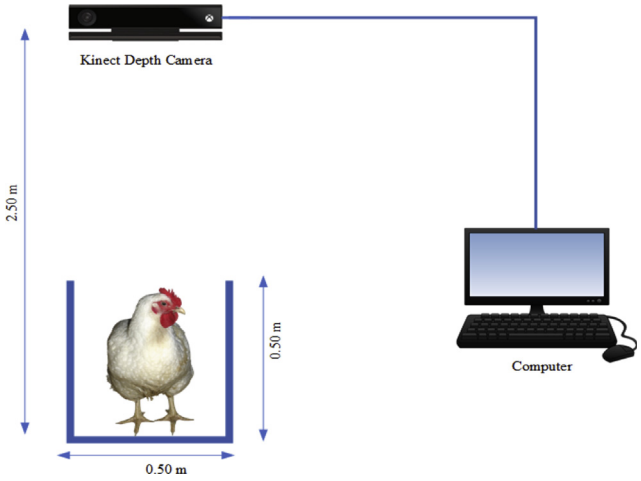

Fig. 1 – Experiment setup and image acquisition system.

Fig. 2 – Colour images of broiler chicken (a) top view and (b) side view during the experiment. (For interpretation of the references to color in this figure legend, the reader is referred to the Web version of this article).

(NDV) with a titre of 10^6 EID_{50} per bird. The NDV was obtained from Nanjing Agricultural University, College of Animal Research and was propagated in 10-day-old specific-pathogen-free (SPF) embryonated chicken eggs (ECEs), following the study of Mast et al. (2006). The second group was used as the control group (G_C). In each experiment, a bird was placed at the starting point of the testing corridor, and overhead depth images of the experimental setup were captured while the broiler walked from the starting point to the end of the testing corridor. This procedure was repeated for all the chickens in each chamber daily. To prevent the chicken from ground pecking and to attract them to walk through the test corridor, the corridor's floor was kept clean at all times, and some feed and a few chickens were placed at the opposite end of the test corridor. Thus, the broiler under test would walk through to join them due to social attraction to cluster together (Febrer, Jones, Donnelly, & Dawkins, 2006).

During the experiment period, overhead images were acquired, and clinical symptoms observed for all the chicken for 14 days (35 days old) with Day 0 being the NDV inoculation day. All experiments were carried out in Nanjing Agricultural University facilities, in compliance with and using protocols (protocol JX524203/1) approved by the Biosafety Committee of Nanjing Agricultural University. The handling of the broiler chicken was performed according to the guidelines approved by the experimental animal administration and ethics committee of Nanjing Agricultural University.

2.2. Data labelling

All the acquired depth data for both sick and healthy birds were manually labelled by surveillance video observation. The timestamps of the moment a broiler entered and exited the test corridor were also labelled for chicken walk speed extraction.

2.3. Image pre-processing and feature extraction algorithms

These algorithms aimed at detecting the health condition of a broiler chicken were based on the walk-speed (γ_s) and simple 2D posture shape descriptors (S_t). Comparison with the video observation was used to validate the proposed health classifier. Additionally, the effect of disease progression (time in days after challenge) on the extracted features was analysed to establish the earliest possible time an infection manifested itself through the extracted feature variables (P_t), where $\gamma_s \in P_t$ and $S_t \in P_t$.

Feature extraction was performed by image analysis on the processed depth images. Health classifier models were then developed, to determine the model performance difference between mobility feature γ_s and image features S_t. Two sets of models were developed; one based solely on S_t (mdl_1) while the other was a combination of all the feature variables (mdl_2). The algorithm flow diagram of the proposed system is presented in Fig. 3.

2.3.1. Image pre-processing algorithm

A raw depth image data was processed as follows. Firstly, background removal by image subtraction technique was performed to remove the floor and test corridor according to Eq. (1).

$$G_{x,y} = \begin{cases} 0 \\ F_{x,y} \end{cases}, \quad \begin{matrix} if\,|F_{x,y} - B_{x,y}| \le T \\ otherwise \end{matrix} \tag{1}$$

where, $G_{x,y}$ is the resultant image with background removed, $F_{x,y}$ is the original image, $B_{x,y}$ is the background image, and T is the threshold. Secondly, based on distance intensities of the depth image (Jana, 2012), maximum and minimum thresholds were set to remain within the Region of Interest (ROI) as presented in Eq. (2).

$$H_{x,y} = \begin{cases} G_{x,y} \\ 0 \end{cases}, \quad \begin{matrix} if\ T_{mn} \le G_{x,y} \le T_{mx} \\ otherwise \end{matrix} \tag{2}$$

where, $H_{x,y}$ is the resultant depth image after depth threshold, T_{mn} is the minimum depth distance threshold, and T_{mx} is the maximum depth distance threshold. Thirdly, $H_{x,y}$ was smoothed by 5×5 pixels zero-mean Gaussian kernel filter (Eq. (3)) then morphological opening (Eq. (4)) was performed by a circular structural element of size 12 pixels to remove local minima associated with both head and body and to obtain a clear depth image. Finally, the image was then converted to a binary image by Otsu's method (Otsu, 1979).

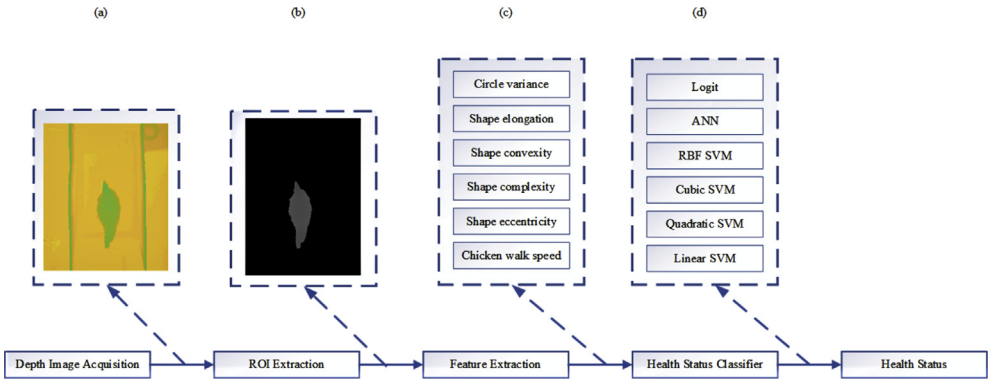

Fig. 3 – The algorithm flow diagram of the proposed system. (a) acquired depth image, (b) segmented broiler image, (c) extracted feature variables, and (d) developed models.

$$I_{x,y} = [H_{x,y}] \otimes \omega \tag{3}$$

where, $I_{x,y} = I(x,y) = I$ is the resultant filtered image, and $\omega = \omega(s,t) = \left(\frac{1}{2\pi\sigma^2} e^{-\frac{1}{2}\left(\frac{s^2+t^2}{\sigma^2}\right)} \right)$ is the Gaussian filter kernel.

$$A_{x,y} = I \bullet Se = (I \oplus Se)\theta Se = \cup\{((Se)_z | (Se)_z)\} \tag{4}$$

where, $A_{x,y}$ is the resultant opened image, Se is the structural element, $(Se)_z$ is the translation of Se by a point z.

2.3.2. *Feature extraction algorithm*

From previous studies on the application of computer vision in livestock image analysis, several image-related features have been proposed and applied to develop correlations to a targeted bio-response or a bio-process (Mollah, Hasan, Salam, & Ali, 2010; Mortensen et al., 2016). However, the proposed technique approaches image analysis from a shape representation point of view by extracting S_t (Zhang & Lu, 2004) also known as shape geometric parameters (Kurnianggoro & Jo, 2018) for correlation to the broiler health status. For each bird, ten images were selected for feature extraction. The equations for the extraction of P_t are summarised in Table 1, while the extraction of S_t from a processed depth image is presented in Fig. 4.

Circle variance also known as circularity (γ_c) (Eq. (5)) is a parameter that presents the degree of similarity of a shape to a circle. The terms $\mu_P = \frac{1}{k}\sum_{i=1}^{k-1}\rho_i$ and $\sigma_P = \sqrt{\frac{1}{k}\sum_{i=1}^{k-1}(\rho_i - \mu_P)^2}$ are the mean and standard deviation of radial distances from the centre of gravity (g) to the shape boundary points (bp) of the 2D shape respectively, $\rho_i = ||bp_i - g||$ is the radial distance of the i^{th} bp from g and k is the total number of bp. Shape Elongation (γ_E) (Eq. (6)) is a parameter based on a shape's minimum bounding box, it represents the degree of stretch, where R_L and R_W are the length and width of the minimum bounding rectangle, respectively. Shape convexity (γ_{cv}) (Eq. (7)) is a parameter related to the shape convex hull in terms of the perimeter. It presents the degree of shape convexity in an epigraph, where P_H is the convex hull perimeter and P_S is the 2D shape perimeter.

The measure of shape complexity (γ_{cx}) (Eq. (8)) was based on the study by Panagiotakis and Argyros (2016), whereby shape complexity is defined as a function of the entropy of the extracted Medial Axis Transform (MAT) 16-bin histograms, where $|W|$ is the number of edges contained in the shape's MAT graph, p_{ij} is the j^{th} bin of the i^{th} histogram and S is the skeleton hence $\log|S|$ represents the global information of the skeleton. The MAT is a locus of centroids and their radii describing maximal circles contained in a shape and are tangent to the shape's boundary points (Zhang & Lu, 2004) as shown in Fig. 4 (c) and (d). Eccentricity (γ_e) (Eq. (9)) is the ratio of the Eigenvalues (λ_1 and λ_2) of a covariance matrix of a fitted ellipse over a 2D shape, and these Eigenvalues correspond to the ellipse's major and the minor axis respectively. Chicken walk speed (γ_S) (Eq. (10)) is the average speed at which the broiler walked from the start to the end of the test corridor. Since the depth data were acquired at 1 fps, t_k was equal to the number of frames captured for the k^{th} chicken, and l being the length of the test corridor.

Table 1 – The extracted features variables.

Extracted Features	Defining Equations	
Circle variance	$\gamma_c = \frac{\sigma_P}{\mu_P}$	(5)
Shape elongation	$\gamma_E = \frac{R_L}{R_W}$	(6)
Shape convexity	$\gamma_{cv} = \frac{P_H}{P_S}$	(7)
Shape complexity	$\gamma_{cx} = -\sum_{i=1}^{|W|}\sum_{j=1}^{16}(p_{ij}\log p_{ij} + \log\|S\|)$	(8)
Shape eccentricity	$\gamma_e = \frac{\lambda_1}{\lambda_2}$	(9)
Chicken walk speed (m s^{-1})	$\gamma_s = \frac{l}{t_k}$	(10)

2.4. *Health status prediction algorithm*

To predict the health status of the broilers, six prediction models were explored. The models were developed based on P_t. The summary of the dataset used in this study is given in Table 2. The dataset was selected based on the criteria that the entire broiler image must be within the screen field and does not touch any of the image borders. A total of 34,280 images were used in this study. The training set was 70% of the total dataset while the remaining 30% as the testing set.

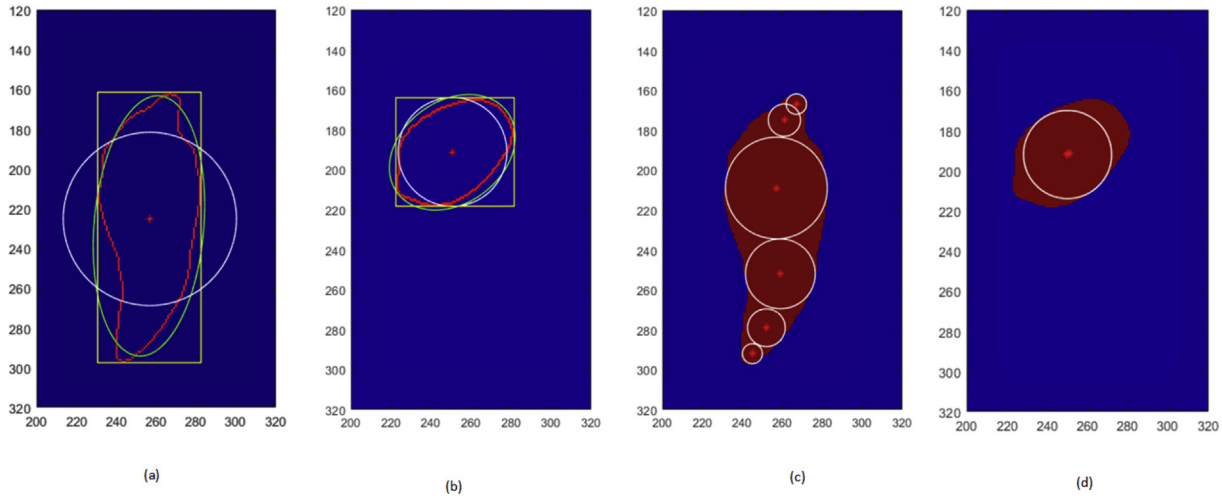

Fig. 4 – The extraction of 2D broiler posture shape parameters: (a) and (b) extraction of circle variance (white circle), shape elongation (yellow rectangle), and eccentricity (green ellipse) on a 2D broiler posture shapes of a broiler in the control group (G_C) and treatment group (G_T), respectively. (c) and (d) extraction of shape complexity on a 2D broiler posture shapes of a broiler in the control group (G_C) and treatment group (G_T) respectively.

Table 2 – Summary of modelling dataset.

Dataset	Number of images
Training dataset	23,996
Testing dataset	10,284
Total dataset	34,280

The explored models were support vector machine (SVM) (linear, quadratic, cubic and radial basis function (RBF)), artificial neural network (ANN), and logit regression. These models were trained by a 10-fold cross-validation-based parameter search on the training dataset after which they were evaluated on a testing dataset. A comparison to the manual labelling of the testing dataset was presented in terms of prediction accuracy.

2.5. *Early disease detection*

For early disease detection, the developed system aimed at establishing the point in time at which infection becomes noticeable by analysing the variations or changes in P_t before any death occurs in G_T with reference to G_C. Firstly, a Spearman's Rank–Order correlation test was performed to establish the direction (positive or negative) of the association between P_t and time after challenge in G_T. Secondly, the Friedman test (Friedman, 1937) also known as Friedman's ANOVA was used to analyse the effect of time on P_t in G_T (grouped into days after challenge). The Friedman test is a non-parametric statistical analysis for variance that avoids the assumption of data normality by comparing columns without the effects of the rows. Hence, size and dependencies do not affect the test results in the test sample (Aydin, 2017a, 2017b; Friedman, 1937). Finally, the Wilcoxon Signed-Rank Test (Taheri & Hesamian, 2013) was applied to determine the statistical differences among the groups (time in days after challenge groupings). This *post hoc* test investigated the changes in rank score between related groups to examine when the differences occur on subsequent group combinations. Note that in this study, the data was not normally distributed even after data transformation. Hence, nonparametric statistical techniques were applied. All statistical computations were performed by Statistical Package for the Social Sciences (IBM SPSS Statistics).

Based on the quartile values of P_t in G_C, and the direction of association of P_t in G_T with time after challenge, a threshold (δ_i) given by Eq. (11) was set on P_t for G_T between Day 3 to Day 7 for early disease detection in G_T i.e., for a +ve r_{si}, P_t values greater than δ_i indicates an infection, while for a -ve r_{si}, P_t values less than δ_i indicates an infection.

$$\delta_i = \begin{cases} Max_{P_{ti}} & if\ r_{si}\ is + ve \\ Min_{P_{ti}} & otherwise \end{cases} \qquad i = 1, 2, \ldots, N \tag{11}$$

where δ_i is the threshold value for the i^{th} feature variable in P_t, N is the total number of feature variables in P_t ($N = 6$), $Max_{P_{ti}}$ and $Min_{P_{ti}}$ are the 3rd quartile and 1st quartile value of the i^{th} feature variable in P_t for G_C as given in Table 7, and r_{si} is the coefficient of correlation of the i^{th} P_t and time (computed from Spearman's Rank–Order correlation test). Note that the quartiles were selected as the threshold values as a precaution against outliers in the minimum–maximum margins.

3. Results

During the 14 days of observation and data collection after NDV challenge, 99.29% of all the chickens in G_T died, as shown in Table 3. The clinical signs observed on the infected birds included respiratory distress, paralysis, circling, and torticollis. Manual verification by surveillance video observation established that the image acquisition system correctly captured the depth images at 1 fps as the broilers walked through the test corridor.

Table 3 – Summary of the performance of the treatment group (G_T) after NDV challenge.

Day after exposure	Number of Broilers			
	Alive	Able to walk	Unable to walk	Dead
0	140	140	0	0
1	140	140	0	0
2	140	140	0	0
3	140	140	0	0
4	140	140	0	0
5	140	140	0	0
6	140	138	2	0
7	138	134	4	2
8	124	99	25	14
9	105	80	25	19
10	77	45	32	28
11	36	7	29	41
12	6	2	4	30
13	2	0	2	4

3.1. *Shape geometric features and mobility feature evaluation*

The P_t were extracted from all the selected images for both sick and healthy birds. The trend of P_t in terms of the mean and range between minimum and maximum (error) values are presented in Fig. 5 for the entire observation period. Generally, it was observed that γ_c and γ_{cv} increased while γ_E, γ_{cx}, γ_e, and γ_s decreased with infection progression (exposure time). From Fig. 5 the sharp rise or drop in the values of G_T features as from around the 6th to the 8th day represents the point at which the infection starts to be manifested by a wide variation in P_t.

At the start of the experiment, ground pecking and preening behaviours by the birds were observed based on the ethogram presented by Pereira et al. (2013) and Kristensen et al. (2007). However, these behaviours were minimised in the preceding experiments by increasing the number of chickens used for social attraction as a motivation for the broiler under test to cluster with the others (Aydin, 2017b; Febrer et al., 2006). However, as shown in Fig. 6, a distinction between healthy birds in G_C ground pecking and infected birds in G_T can be characterised by the tail positioning, whereby in the former during ground pecking activity the tail is usually not dropped. Furthermore, several images of a single bird were acquired as it walked through the test corridor, thus, minimised the errors associated with the mismatch between ground pecking and sick broilers in the classification.

3.2. *Health status classifier evaluation*

The model parameters for all the trained models developed in this study are presented in Table 4. Classifier parameters are important factors that affect the overall performance of a model in terms of efficiency and accuracy. The choice of the kernel function is a critical factor in performance of an SVM model (Zhuang et al., 2018). The commonly applied kernel functions are the linear, polynomial (quadratic and cubic) and the RBF kernel functions. The logit regression predicts probabilities rather than grouping data into classes. Therefore, it's often fitted using a likelihood function, which is a maximisation problem (General Maximum Likelihood (GML)). Therefore, the estimation of this maximum likelihood significantly affects the overall model performance (Kleinbaum & Klein, 2010; Mansournia, Geroldinger, Greenland, & Heinze, 2017). The SVM kernel functions and the logit log(likelihood) parameters were computed iteratively during the 10-fold-validation in the model training phase (parameters resulting to highest validation accuracy while effectively avoiding overfitting and underfitting of a model and having a good generalisation ability). Similarly, for the ANN model, the number of neurons in the hidden layers was set to 12 after evaluation of the percent error during model validation. However, as the number of neurons increases, percentage error decreases at the expense of the computation time (Wongsriworaphon et al., 2015). Therefore, in this current study, the number of hidden layers was set to 12 to balance the computation time and percentage error while training was performed by scaled conjugate gradient backpropagation algorithm (Møller, 1993).

All models were evaluated on the testing dataset. Table 5 presents the performance of the models on the testing dataset in terms of accuracy. It was established that RBF-SVM had the best classification results while Logit regression returned the lowest accuracy irrespective of the training features. There was no significant performance difference between mdl_1 and mdl_2. However, mdl_2 was slightly more accurate than mdl_1 for all the developed models.

Additionally, the performance of each model was evaluated based on the relative error of daily testing dataset, as shown in Fig. 7. It was established that all the models had similar performance except for the cubic SVM in mdl_1. Furthermore, it was observed that the cubic SVM had the largest variations in its accuracy when mdl_1 and mdl_2 performances were compared on the entire testing dataset as presented in Table 5.

3.3. *Early disease detection by statistical analysis*

A correlation analysis established that there was a statistically significant ($p < 0.01$) positive correlation between both γ_c and γ_{cv} with time in days after challenge with coefficients $r_s = 0.883$ and 0.596, respectively. However, it was established that there was a statistically significant ($p < 0.01$) negative correlation between γ_E, γ_{cx}, γ_e, and γ_s with time after challenge, with coefficients $r_s = 0.872$, 0.695, 0.757, and 0.838 respectively. This correlation test result concurs with the visual observations made on the trends of P_t as presented in Fig. 5. Table 6 and Fig. 8 presents the statistical analysis of P_t for the G_T while Table 7 presents the descriptive statistics of P_t for G_C for the entire experiment period. The statistical analysis for G_T was performed as from Day 3 till Day 7 when the first broiler death occurred to eliminate the effects of the NDV inoculation procedure on the G_T broilers during Day 0 to Day 2 (effect of injection), while Day 7 was included for comparison purposes.

By Friedman's test, there was a statistically significant difference ($p < 0.05$) in all the P_t depending on the time after NDV challenge. A *post hoc* test on combinations of Day 3 to Day 4, Day 4 to Day 5, and Day 5 to Day 6 was performed to

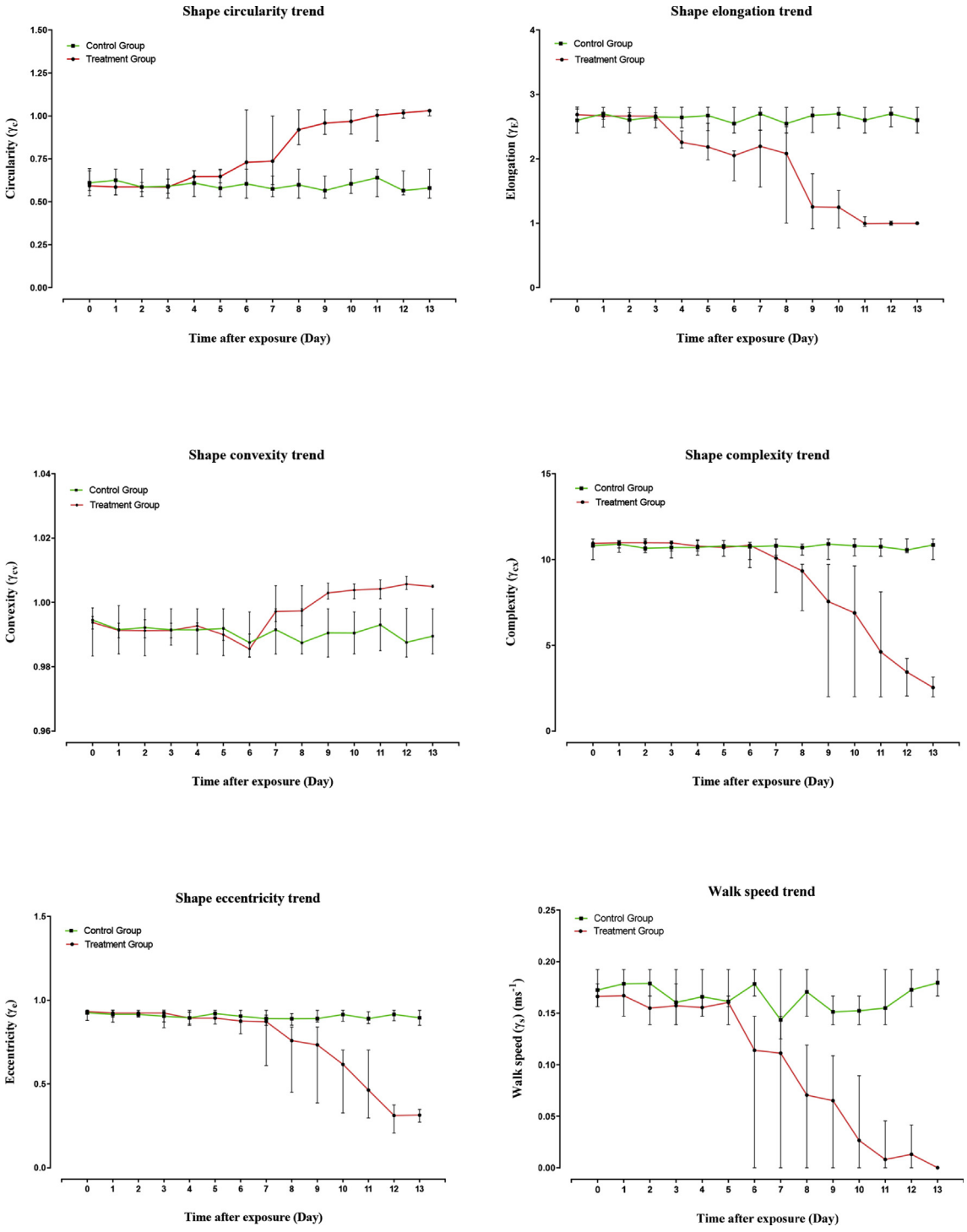

Fig. 5 – The mean, maximum and minimum daily trend of the extracted feature variables during the observation period for both the control group (G_C) and treatment group (G_T) broilers.

examine where the differences occur. Based on the study by Glickman, Rao, and Schultz (2014), it was not necessary to perform Bonferroni adjustment to prevent a deleterious effect on the statistical inference (Perneger, 1998).

According to Table 6, the mean values of γ_c on Days 4–7 were significantly ($p < 0.05$) greater than the γ_c mean for Day 3. However, there were no statistically significant ($p < 0.05$) differences between Days 4 and 5 nor between Days 6 and 7 in terms of γ_c mean values. The mean values of γ_E on Days 4–7 were significantly ($p < 0.05$) lower than the γ_E mean for Day 3. Additionally, there was no statistically significant ($p < 0.05$) differences between Days 4, 5 and 7 in terms of γ_E mean values. The mean values of γ_{cv} on Day 7 was significantly ($p < 0.05$) greater than the γ_{cv} mean for Days 3–6. However, there was no statistically significant ($p < 0.05$) differences between Days 3, 4 and 5 in terms of γ_{cv} mean values. The mean

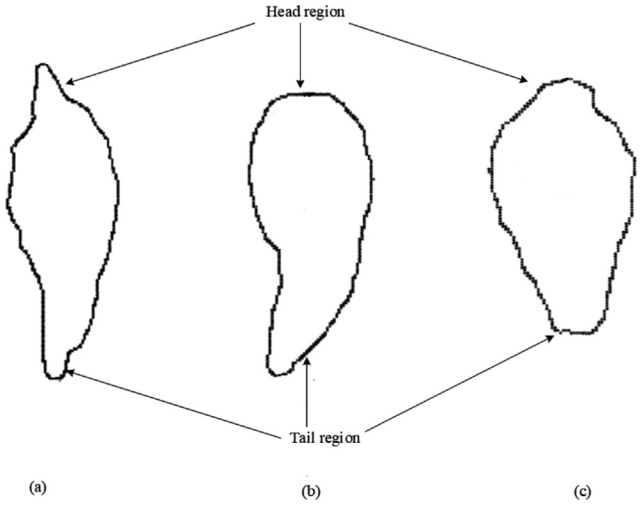

Fig. 6 – An illustration of the differences in the 2D posture shape on Day 7 for (a and b) a control group (G_C) bird in a walking position and in a ground pecking position respectively and (c) a treatment group (G_T) bird in a walking position.

Table 4 – The parameters of the developed recognition models.

Classifier parameters	Mdl_1		Mdl_2	
SVM Kernel parameters	Scale	degree	Scale	degree
Linear	0.4083	–	0.4877	–
Quadratic	0.3871	2	0.4262	2
Cubic	0.3360	3	0.5041	3
RBF	0.5600	–	0.6100	–
Logit log(likelihood)	−9273.413		−8774.085	
ANN topology	5–12 – 2		6–12 – 2	

values of γ_{cx} on Days 4–7 were significantly ($p < 0.05$) lower than the γ_{cx} mean for Day 3. However, there were no statistically significant ($p < 0.05$) differences between Days 4 and 5 in terms of γ_{cx} mean values. The mean values of γ_e on Days 4–7 were significantly ($p < 0.05$) lower than the γ_e mean for Day 3. Furthermore, there was no statistically significant ($p < 0.05$) differences between Days 4 and 5 nor between Days 6 and 7 in terms of γ_e mean values. The mean values of γ_s on Days 6–7 were significantly ($p < 0.05$) lower than the γ_s mean for Days 3–5. However, there were no statistically significant ($p < 0.05$) differences between Days 3 and 4 nor between Days 6 and 7 in terms of γ_s mean values.

Table 5 – Comparison of the performance of different models on the testing dataset (accuracy).

Models	mdl_1	mdl_2
Linear SVM	0.858	0.860
Quadratic SVM	0.961	0.965
Cubic SVM	0.917	0.971
RBF SVM	0.975	0.978
ANN	0.969	0.969
Logit	0.817	0.808

Figure 8 shows the early infection detection based on the above threshold on G_T. It was established that only γ_c, γ_E, γ_e and γ_s could provide an early detection on Days 4, 4, 6 and 6 respectively. However, early detection could not be achieved by γ_{cv} and γ_{cx} before any death occurs in G_T.

4. Discussion

NDV is one of the common poultry diseases (Butcher et al., 1999) caused by NDV Avulavirus (Waterson, Pennington, & Allan, 1967). The housing chambers used during the experiment were completely insulated to prevent inter-group infection because NDV can be propagated by air from one bird to another (Chansiripornchai & Sasipreeyajan, 2006). From Table 3, the severe effects of the infection were apparent from Day 9, but substantial effects in posture and mobility were visible by Day 7. This was due to NDV's short incubation period of 2–15 days (Rahman, Rabbani, Uddin, Chakrabartty, & Her, 2012).

The proposed system introduces an automated monitoring technique of chicken welfare-related bio-responses by a machine vision system. Image preprocessing algorithm was developed as the initial step in the visual diagnosis of broiler disease (Zhuang et al., 2018) to segment the chicken shape from the background. Secondly, S_t were extracted by image analysis algorithm. S_t have description ability and can be used to differentiate shapes in shape analysis, but to achieve a higher discriminative power several S_t are always combined (Kurnianggoro & Jo, 2018; Zhang & Lu, 2004). Therefore, in this proposed technique, S_t was described by five geometric parameters to improve the descriptive ability.

Consider a comparison of G_T to G_C in Fig. 5, the γ_c and γ_{cv} were observed to increase with exposure time from Day 4 and Day 7 respectively, from the observation that an infected chicken displayed a typical sick bird posture-hunched stance, characterised by a tucked-in neck and dropped tail. Hence, the shape of a sick broiler appeared more circular and more convex compared to a healthy broiler with exposure time, as shown in Fig. 4 and Fig. 9. The γ_E, γ_{cx}, and γ_e were observed to decrease with exposure time as from Day 4, Day 7 and Day 8 respectively. γ_E is minimum bounding box dependent, a healthy bird's bounding box has a longer longitudinal length compared to a sick broiler. Hence, the degree of stretch is higher than that of a sick bird. The γ_{cx} adopted in this study is MAT dependent, the more circular a 2D shape is, the fewer the maximal inscribed circles, hence, low shape complexity in sick birds (Fig. 4 c and d). Finally, γ_e is a parameter dependent on an inscribed ellipse on a shape it is the extent to which the fitted ellipse departs from circularity, for a circular shape, γ_e is zero. Thus, sick birds will have a lower eccentricity because their shape has a higher circularity compared to the healthy broiler. Figure 9 presents a comparison of two chickens from each group with their images on Days 0, 4, 7, 10, and 13. A clear visual distinction can be observed as from Day 10, whereby the bird in G_T appears more circular and less elongated than the bird in G_C.

The chicken mobility in terms of γ_s in G_T was observed to decrease from an average of 0.173 m s^{-1} on the day of inoculation (Day 0) to complete immobility with disease progression. Additionally, the average walk speed of G_C was

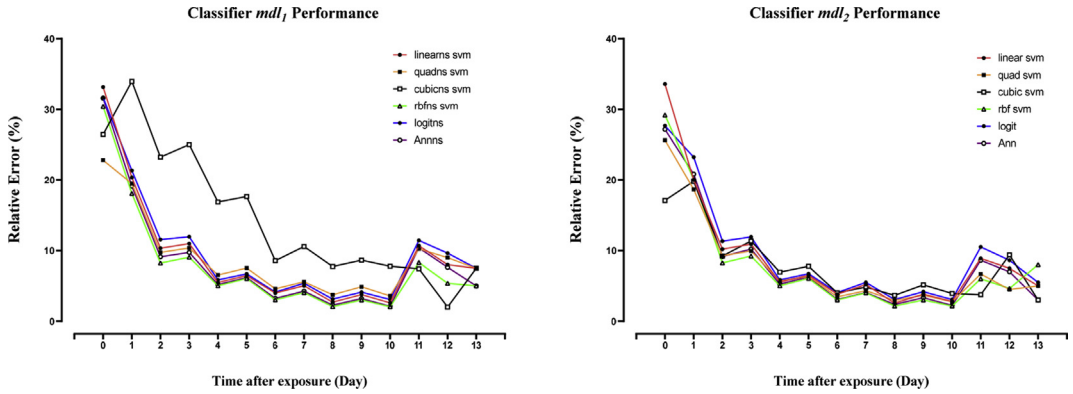

Fig. 7 – The performance of the developed health classifiers on the daily testing dataset.

Table 6 – The statistical results of the P_t of birds in the treatment group (G_T) expressed in mean values for Day 3 to Day 7 after NDV challenge.

Days after exposure	Circularity (γ_c) mean	Elongation (γ_E) mean	Convexity (γ_{cv}) mean	Complexity (γ_{cx}) mean	Eccentricity (γ_e) mean	Walk speed (ms^{-1}) (γ_s) mean
Day 3	0.585^{c}	2.665^{a}	0.991^{b}	10.975^{a}	0.924^{a}	0.157^{b}
Day 4	0.646^{b}	2.256^{b}	0.993^{b}	10.776^{c}	0.893^{b}	0.156^{b}
Day 5	0.647^{b}	2.184^{b}	0.990^{b}	10.701^{c}	0.893^{b}	0.161^{a}
Day 6	0.730^{a}	2.052^{c}	0.986^{c}	10.834^{b}	0.876^{c}	0.114^{c}
Day 7	0.737^{a}	2.195^{b}	0.997^{a}	10.081^{d}	0.872^{c}	0.111^{c}

a, b, c, d Mean ranks within a column, with no superscript in common differ significantly ($p < 0.05$).

0.164 m s^{-1} for the entire experiment period as shown in Table 7. This finding concurs with those of Aydin (2017a), Nääs et al. (2010), and Caplen et al. (2012), that healthy sound birds walk significantly faster between a range of 0.15 m s^{-1} to 0.17 m s^{-1}, while unsound birds walked at a lower speed of below 0.11 m s^{-1}. Additionally, the results obtained in our study concur with these previous reports based on the statistical analysis of γ_s for early disease detection, as presented in Table 6, whereby Day 6 had a mean γ_s of 0.114 m s^{-1} and it is the initial point in time at which some of the broilers were immobile as seen in Table 3.

A comparison of the developed models presented in Table 5 shows that RBF-SVM outperformed all the other models. Additionally, it had a good generalisation ability and robustness on the testing dataset as presented in Fig. 7. However, a high prediction error occurred on the first two days after NDV challenge (Fig. 7), because the NDV was still in its incubation phase. Hence, the birds in G_T had a similar appearance to those in G_C. Thus, infected birds were predicted to belong to G_C. Moreover, this is why Day 0 to Day 2 was not considered in the statistical analysis for early disease detection in Table 6. A comparison of mdl_1 to mdl_2 showed that there was no significant difference between the models in terms of model accuracy. Hence, it can be concluded that S_t can be applied as predictors in broiler disease prediction. Furthermore, γ_s has been applied in several studies to access the gait score (Aydin, 2017a; Caplen et al., 2012), these studies were based on lameness detection and established that sound birds walk significantly faster. Thus, walk speed as a mobility feature can be used as a feature variable in disease detection and prediction systems in birds.

In an efficient and effective disease detection system in poultry production, the occurrence of any infection should be detected before the death of any bird in a flock. Based on the correlation test results, early disease detection could be achieved by establishing the time at which γ_c and γ_{cv} starts to increase, while γ_E, γ_{cx}, γ_e, and γ_s start to decrease before the first broiler death. However, it was established that γ_{cv}, and γ_{cx} could not provide an early detection based on the set threshold technique. Furthermore, from the correlation results γ_{cv} and γ_{cx} had weak correlation strength with time in days after exposure compared to the other feature variables. γ_c and γ_E could provide an early detection on Day 4, while γ_e and γ_s on Day 6. Moreover, from Fig. 8 it can be observed that γ_c (mean and median (IQR)) increases in Day 4 when compared to Day 3. Similarly, γ_E (mean and median (IQR)) decreases in Day 4 when compared to Day 3. Additionally, both γ_s and γ_e (mean and median (IQR)) are also observed to decrease in Day 6 when compared to Day 5. Furthermore, according to Aydin (2017a) the γ_s (mean) for Day 3–5 are considered as γ_s of sound birds while γ_s (mean) for Day 6 would be considered as γ_s of unsound birds. It was also noted that the infection could only be detected after the incubation period of the NDV Avulavirus. The P_t of some days after challenge (Day 4 and 5 for γ_c and γ_E, Day 3, 4, 5 and 6 for γ_{cv}, and Day 3 and 4 for γ_s) were quite similar as seen in Table 6. Therefore, accurate detection of variation of feature variables on these days would be quite difficult. Hence, for precise identification of the effect of an infection on P_t on these days, a new feature should be included in the proposed system or the system should be integrated with other welfare, bio-response related monitoring systems such as weight estimation or activity detection.

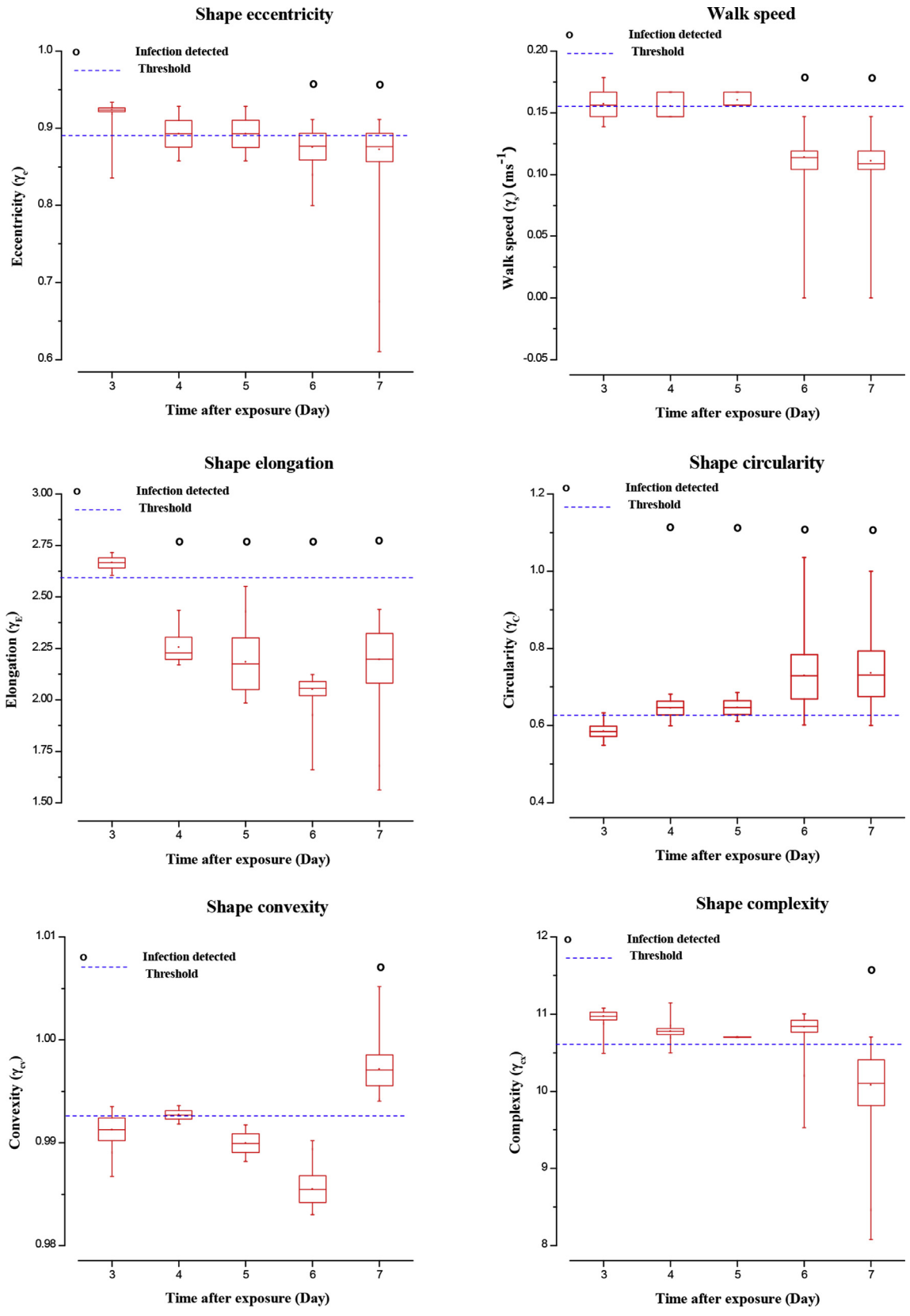

Fig. 8 – The box plots presenting the statistical analysis for the extracted feature variables for Day 3 till Day 7, the thresholds for infection detection and the detected infection days in the treatment group (G_T).

Table 7 – The descriptive statistic for the P_t of birds in the control group (G_C) for the entire experiment period (n = 19,580).

Feature variables	sCircularity	Elongation	Convexity	Complexity	Eccentricity	Walk speed (ms^{-1})
(P_t)	(γ_c)	(γ_E)	(γ_{cv})	(γ_{cx})	(γ_e)	(γ_s)
Minimum	0.520	2.400	0.983	9.994	0.850	0.125
Maximum	0.690	2.802	0.999	11.200	0.940	0.192
Mean	0.595	2.639	0.991	10.760	0.905	0.164
1st Quartile	0.563	2.592	0.988	10.606	0.890	0.156
3rd Quartile	0.626	2.711	0.993	10.900	0.922	0.179
Median	0.5911	2.652	0.991	10.751	0.908	0.167
Standard deviation	4.100×10^{-2}	9.800×10^{-2}	3.505×10^{-3}	2.036×10^{-1}	2.140×10^{-2}	1.992×10^{-2}
Variance	1.679×10^{-3}	9.604×10^{-3}	1.229×10^{-5}	4.145×10^{-2}	4.580×10^{-4}	3.968×10^{-4}
Standard error	2.928×10^{-4}	7.004×10^{-4}	2.505×10^{-5}	1.455×10^{-3}	1.529×10^{-4}	1.424×10^{-4}

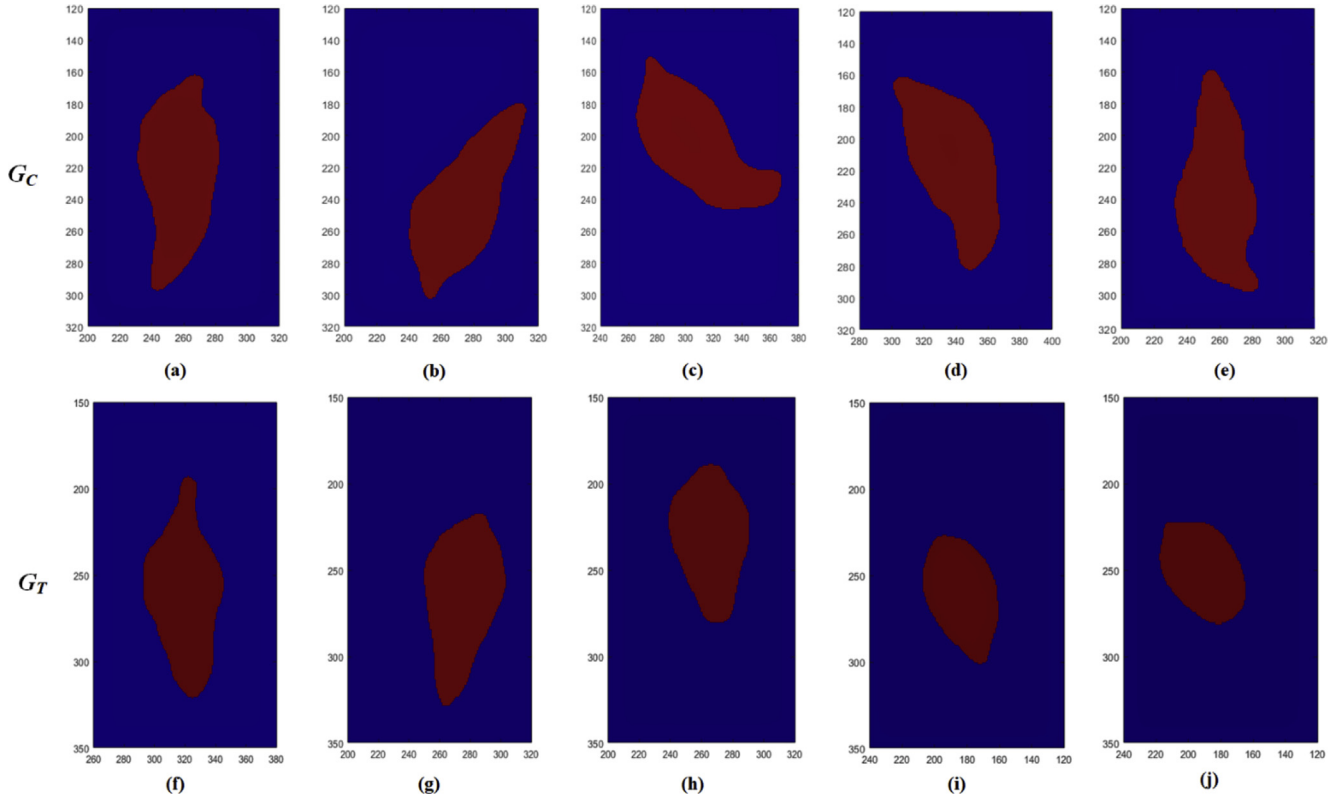

Fig. 9 – Observed shape changes with exposure time of two birds, i.e., a control group (G_C) and a treatment group (G_T), (a and f) Day 0, (b and g) Day 4, (c and h) Day 7, (d and i) Day 10, and (e and j) Day 13.

Finally, the proposed monitoring system not only provides early detection and prediction of disease occurrence but can also automatically, continuously and non-intrusively take measurements throughout the lifespan of the birds. Thus, reduced surveillance costs would benefit both the broiler and poultry producer.

5. Conclusions

This study proposes an early detection and prediction of a disease occurrence in broiler chicken based on S_t, and γ_s. The variations of the extracted features variables were analysed in terms of time after exposure to an infection and correlations to the health status were developed. The results obtained suggest that the proposed machine vision system can provide an early disease detection and prediction in broiler chicken. However, this system needs to be validated on different types of chicken breeds and infection types. Despite these limitations, the proposed technique with acceptable results achieved the objectives of this research study. It is of great importance to detect an infection in a flock in a timely manner to allow stockmen and veterinarians to take necessary actions to prevent huge loses and to keep a good animal welfare

status. Thus, this proposed system can be applied as a PLF monitoring system for the entire life span of broilers. Additionally, this system can be integrated with other bio-response monitoring systems such a lameness detection, weight estimation, activity level, and behaviour detection systems in a broiler chicken management system.

Acknowledgments

The project was funded by China National Key Research and Development project (Grant N°. 2017YFE0114400).

REFERENCES

Aydin, A. (2017a). Development of an early detection system for lameness of broilers using computer vision. *Computers and Electronics in Agriculture, 136*, 140–146. https://doi.org/10.1016/j.compag.2017.02.019.

Aydin, A. (2017b). Using 3D vision camera system to automatically assess the level of inactivity in broiler chickens. *Computers and Electronics in Agriculture, 135*, 4–10. https://doi.org/10.1016/j.compag.2017.01.024.

Bradshaw, R. H., Kirkden, R. D., & Broom, D. M. (2002). A review of the aetiology and pathology of leg weakness in broilers in relation to welfare. *Avian and Poultry Biology Reviews, 13*(2), 45–103. https://doi.org/10.3184/147020602783698421.

Butcher, G. D., Jacob, J. P., & Mather, F. B. (1999). *Common poultry diseases. PS47-Series of the veterinary medicine-large animal clinical Sciences department, UF/IFAS extension*. Retrieved from: https://edis.ifas.ufl.edu/pdffiles/PS/PS04400.pdf.

Caplen, G., Hothersall, B., Murrell, J. C., Nicol, C. J., Waterman-Pearson, A. E., Weeks, C. A., et al. (2012). Kinematic analysis quantifies gait abnormalities associated with lameness in broiler chickens and identifies evolutionary gait differences. *PLoS One, 7*(7), e40800. https://doi.org/10.1371/journal.pone.0040800.

Chansiripornchai, N., & Sasipreeyajan, J. (2006). Efficacy of live B1 or Ulster 2C Newcastle disease vaccines simultaneously vaccinated with inactivated oil adjuvant vaccine for protection of Newcastle disease virus in broiler chickens. *Acta Veterinaria Scandinavica, 48*(1), 2. https://doi.org/10.1186/1751-0147-48-2.

Damerow, G. (2016). *The chicken health Handbook: A complete guide to maximizing flock health and dealing with disease*. Storey Publishing.

Febrer, K., Jones, T. A., Donnelly, C. A., & Dawkins, M. S. (2006). Forced to crowd or choosing to cluster? Spatial distribution indicates social attraction in broiler chickens. *Animal Behaviour, 72*(6), 1291–1300. https://doi.org/10.1016/j.anbehav.2006.03.019.

Friedman, M. (1937). The use of ranks to avoid the assumption of normality implicit in the analysis of variance. *Journal of the American Statistical Association, 32*(200), 675–701. https://doi.org/10.1080/01621459.1937.10503522.

Friel, S., & Ford, L. (2015). Systems, food security and human health. *Food Security, 7*(2), 437–451. https://doi.org/10.1007/s12571-015-0433-1.

Glickman, M. E., Rao, S. R., & Schultz, M. R. (2014). False discovery rate control is a recommended alternative to Bonferroni-type adjustments in health studies. *Journal of Clinical Epidemiology, 67*(8), 850–857. https://doi.org/10.1016/j.jclinepi.2014.03.012.

Henchion, M., McCarthy, M., Resconi, V. C., & Troy, D. (2014). Meat consumption: Trends and quality matters. *Meat Science, 98*(3), 561–568. https://doi.org/10.1016/j.meatsci.2014.06.007.

Huang, J., Wang, W., & Zhang, T. (2019). Method for detecting avian influenza disease of chickens based on sound analysis. *Biosystems Engineering, 180*, 16–24. https://doi.org/10.1016/j.biosystemseng.2019.01.015.

Jana, A. (2012). *Kinect for windows SDK programming guide*. Packt Publishing Ltd.

Kleinbaum, D. G., & Klein, M. (2010). Maximum likelihood techniques: An overview. In *Logistic regression* (pp. 103–127).

Kongsro, J. (2014). Estimation of pig weight using a Microsoft Kinect prototype imaging system. *Computers and Electronics in Agriculture, 109*, 32–35. https://doi.org/10.1016/j.compag.2014.08.008.

Kristensen, H. H., & Cornou, C. (2011). Automatic detection of deviations in activity levels in groups of broiler chickens—a pilot study. *Biosystems Engineering, 109*(4), 369–376. https://doi.org/10.1016/j.biosystemseng.2011.05.002.

Kristensen, H. H., Prescott, N. B., Perry, G. C., Ladewig, J., Ersbøll, A. K., Overvad, K. C., et al. (2007). The behaviour of broiler chickens in different light sources and illuminances. *Applied Animal Behaviour Science, 103*(1–2), 75–89. https://doi.org/10.1016/j.applanim.2006.04.017.

Kurnianggoro, L., & Jo, K.-H. (2018). A survey of 2D shape representation: Methods, evaluations, and future research directions. *Neurocomputing, 300*, 1–16. https://doi.org/10.1016/j.neucom.2018.02.093.

Manning, L., Chadd, S. A., & Baines, R. N. (2007). Key health and welfare indicators for broiler production. *World's Poultry Science Journal, 63*(1), 46–62. https://doi.org/10.1017/S0043933907001262.

Mansournia, M. A., Geroldinger, A., Greenland, S., & Heinze, G. (2017). Separation in logistic regression: Causes, consequences, and control. *American Journal of Epidemiology, 187*(4), 864–870. https://doi.org/10.1093/aje/kwx299.

Mast, J., Nanbru, C., Decaesstecker, M., Lambrecht, B., Couvreur, B., Meulemans, G., et al. (2006). Vaccination of chicken embryos with escape mutants of La Sota Newcastle disease virus induces a protective immune response. *Vaccine, 24*(11), 1756–1765. https://doi.org/10.1016/j.vaccine.2005.10.020.

Menesatti, P., Costa, C., Antonucci, F., Steri, R., Pallottino, F., & Catillo, G. (2014). A low-cost stereovision system to estimate size and weight of live sheep. *Computers and Electronics in Agriculture, 103*, 33–38. https://doi.org/10.1016/j.compag.2014.01.018.

Mollah, M. B. R., Hasan, M. A., Salam, M. A., & Ali, M. A. (2010). Digital image analysis to estimate the live weight of broiler. *Computers and Electronics in Agriculture, 72*(1), 48–52. https://doi.org/10.1016/j.compag.2010.02.002.

Møller, M. F. (1993). A scaled conjugate gradient algorithm for fast supervised learning. *Neural Networks, 6*(4), 525–533. https://doi.org/10.1016/S0893-6080(05)80056-5.

Mortensen, A. K., Lisouski, P., & Ahrendt, P. (2016). Weight prediction of broiler chickens using 3D computer vision. *Computers and Electronics in Agriculture, 123*, 319–326. https://doi.org/10.1016/j.compag.2016.03.011.

de Nääs, I. A., de Paz, I. C. L. A., Baracho, M., dos, S., de Menezes, A. G., de Lima, K. A. O., et al. (2010). Assessing locomotion deficiency in broiler chicken. *Scientia Agricola, 67*(2), 129–135. https://doi.org/10.1590/S0103-90162010000200001.

OECD-FAO. (2017). *Organisation for economic Co-operation and development (OECD)/Food and agriculture organization of the United Nations (FAO). 2017. Agricultural outlook 2017–2026: Special Focus: Southeast Asia*. Retrieved from: http://www.fao.org/3/a-i7465e.pdf.

Okinda, C., Lu, M., Nyalala, I., Li, J., & Shen, M. (2018). Asphyxia occurrence detection in sows during the farrowing phase by inter-birth interval evaluation. *Computers and Electronics in Agriculture, 152*, 221–232. https://doi.org/10.1016/j.compag.2018.07.007.

Otsu, N. (1979). A threshold selection method from gray-level histograms. *IEEE Transactions on Systems, Man, and Cybernetics, 9*(1), 62–66. https://doi.org/10.1109/TSMC.1979.4310076.

Panagiotakis, C., & Argyros, A. (2016). Parameter-free modelling of 2D shapes with ellipses. *Pattern Recognition, 53*, 259–275. https://doi.org/10.1016/j.patcog.2015.11.004.

Paul-Murphy, J. R., & Hawkins, M. (2014). Bird-specific considerations: Recognizing pain behavior in pet birds. In *Handbook of veterinary pain management* (3rd ed., pp. 536–554).

Peiris, J. S. M., Cowling, B. J., Wu, J. T., Feng, L., Guan, Y., Yu, H., et al. (2016). Interventions to reduce zoonotic and pandemic risks from avian influenza in Asia. *The Lancet Infectious Diseases, 16*(2), 252–258. https://doi.org/10.1016/S1473-3099(15)00502-2.

Pereira, D. F., Miyamoto, B. C. B., Maia, G. D. N., Sales, G. T., Magalhães, M. M., & Gates, R. S. (2013). Machine vision to identify broiler breeder behavior. *Computers and Electronics in Agriculture, 99*, 194–199. https://doi.org/10.1016/j.compag.2013.09.012.

Perneger, T. V. (1998). What's wrong with Bonferroni adjustments. *BMJ, 316*(7139), 1236–1238. https://doi.org/10.1136/bmj.316.7139.1236.

Rahman, S., Rabbani, M. G., Uddin, M. J., Chakrabartty, A., & Her, M. (2012). Prevalence of avian influenza and Newcastle disease viruses using rapid antigen detection Kit in poultry in some areas of Bangladesh. *Archives of Clinical Microbiology, 3*(1). https://doi.org/10.3823/248.

Rushton, J., Viscarra, R., Bleich, E. G., & McLeod, A. (2005). Impact of avian influenza outbreaks in the poultry sectors of five South East Asian countries (Cambodia, Indonesia, Lao PDR, Thailand, Viet Nam) outbreak costs, responses and potential long term control. *World's Poultry Science Journal, 61*(3), 491–514. https://doi.org/10.1079/WPS200570.

Sims, L. D. (2008). Risks associated with poultry production systems. *International Conference Poultry in the Twenty-First Century, 1*, 24. Retrieved from: http://www.fao.org/WAICENT/FAOINFO/AGRICULT/againfo/home/events/bangkok2007/docs/part2/2_1.pdf.

Tablante, N. L. (2013). *Common poultry diseases and their prevention*. University of Maryland Extension. Retrieved from: https://extension.umd.edu/sites/extension.umd.edu/files/_docs/Common-Poultry-Diseases-and-Their-Prevention_Tablante_2013.pdf.

Taheri, S. M., & Hesamian, G. (2013). A generalization of the Wilcoxon signed-rank test and its applications. *Statistical Papers, 54*(2), 457–470. https://doi.org/10.1007/s00362-012-0443-4.

Thorp, B. H., & Duff, S. R. I. (1988). Effect of exercise on the vascular pattern in the bone extremities of broiler fowl. *Research in Veterinary Science, 45*(1), 72–77. https://doi.org/10.1016/S0034-5288(18)30897-X.

Van der Stuyft, E., Schofield, C. P., Randall, J. M., Wambacq, P., & Goedseels, V. (1991). Development and application of computer vision systems for use in livestock production. *Computers and Electronics in Agriculture, 6*(3), 243–265. https://doi.org/10.1016/0168-1699(91)90006-U.

Waterson, A. P., Pennington, T. H., & Allan, W. H. (1967). Virulence in Newcastle disease virus: A preliminary study. *British Medical Bulletin, 23*(2), 138–143. https://doi.org/10.1093/oxfordjournals.bmb.a070534.

Welfare Quality®. (2009). Welfare Quality® assessment protocol for poultry (broilers, laying hens). In *Welfare Quality® consortium, Lelystad, Netherlands* (p. 114pp). Retrieved from: http://edepot.wur.nl/233471.

Wongsriworaphon, A., Arnonkijpanich, B., & Pathumnakul, S. (2015). An approach based on digital image analysis to estimate the live weights of pigs in farm environments. *Computers and Electronics in Agriculture, 115*, 26–33. https://doi.org/10.1016/j.compag.2015.05.004.

Zhang, D., & Lu, G. (2004). Review of shape representation and description techniques. *Pattern Recognition, 37*(1), 1–19. https://doi.org/10.1016/j.patcog.2003.07.008.

Zhuang, X., Bi, M., Guo, J., Wu, S., & Zhang, T. (2018). Development of an early warning algorithm to detect sick broilers. *Computers and Electronics in Agriculture, 144*, 102–113. https://doi.org/10.1016/j.compag.2017.11.032.

Zhuang, X., & Zhang, T. (2019). Detection of sick broilers by digital image processing and deep learning. *Biosystems Engineering, 179*, 106–116. https://doi.org/10.1016/j.biosystemseng.2019.01.003.